

## CURRENT-MODE SIGNAL PROCESSING CIRCUITS

Vello MÄNNAMA

Department of Electronics, Tallinn Technical University, Ehitajate tee 5, EE-0026 Tallinn, Estonia;  
e-mail: vellom@edu.ttu.ee

Received 30 May 1997

**Abstract.** This paper presents a short overview of current-mode signal processing principles and their implementation in modern circuit design. The translinear principles for bipolar structures are explained. Main properties of the static and dynamic current mirrors are described. The theoretical basis of current conveyors (CC) is given, and an implementation of CC with a “diamond” structure is demonstrated. The current-feedback operational amplifier, as a versatile circuit component with high speed and slew rate, is analyzed.

Implementation of the current-mode approach in order to improve the dynamic behaviour of precise rectification is discussed. A modified bridge bias arrangement is presented for a precision current-mode rectifier that avoids the adjustment sensitivity, and current-mode bridge rectification is analyzed. An improved all-conveyor current-mode wideband rectifier design is described, which can also be used in high-speed balanced modulators.

**Key words:** current-mode design, translinearity, current mirror, current conveyor, current-feedback operational amplifier, current-mode rectifier, prebiased diode bridge.

### 1. INTRODUCTION

Electronic design has historically been viewed as a voltage-dominated form of signal processing. Generally, current signals are transferred into the voltage domain before any analogue or digital signal processing takes place, although amplifying components – bipolar and FET transistors – are both current output devices. Many primary signal sources (sensors) and actuators are current based.

Modern integrated circuit (IC) design is now able to exploit the potential of current-mode signal processing, providing optimum solutions for many circuit and system problems [1–4]. New and more mature device technologies are

available. In CMOS technology, with mixed analogue and digital circuitry in VLSI, the shrinking feature size necessitates the reduction of supply voltages, and as a consequence, voltage domain behaviour will suffer. Such difficulty can be overcome by operating in the current domain [1]. BiCMOS technology combines both advantages of bipolar and CMOS, for which the current-mode technique is ideally suited. GaAs HBT and MESFET technologies open the possibilities of microwave and optical system design.

Implementation of current-mode techniques facilitates many new, particularly high speed and high operating frequency designs. Current-mode rectifiers [3] have proved to have good dynamic behaviour. A double synchronized current-controlled oscillator of the phase-locked loop frequency synthesizer is described in [5], with an output frequency of about 1 GHz. Current-mode control and steering is also inherent for many power systems [6], e.g. in order to supply gas lasers or maintain a stable magnetic field.

## 2. TRANSLINEARITY

The term “translinear” was first used by B. Gilbert to point out the fact that the transconductance of a bipolar junction transistor (BJT) is linearly proportional to its collector current [7], which immediately results from the exponential dependence between the collector current  $I_c$  and the base-emitter voltage  $V_{be}$ :

$$I_c = I_s \exp(V_{be}/V_T), \quad (1)$$

where  $V_T$  is the thermal voltage (25.85 mV at 300 K) and  $I_s$  is the saturation current. In the reciprocal case

$$V_{be} = V_T \ln(I_c / I_s). \quad (2)$$

The transconductance  $g_m$  of the BJT can be found by differentiating (1) to give

$$g_m = dI_c / dV_{be} = I_c / V_T. \quad (3)$$

It is assumed in Eqs. (1)–(3) that the current gain  $\beta \gg 1$ , which is valid for most practical implementations.

An important role in bipolar circuits is played by closed “translinear” loops that consist of an even number of forward-biased p-n junctions (see Fig. 1), arranged to provide an equal number of clockwise (CW) facing and counter-clockwise (CCW) facing polarities. The sum of the junction voltages is zero, and taking into account (2), then

$$\sum_i V_T \ln(I_{ci} / I_{si}) = \sum_j V_T \ln(I_{cj} / I_{sj}), \quad (4)$$

where subscripts  $i$  and  $j$  mark the CW-faced and CCW-faced junctions (usually base-emitter junctions of BJTs with  $I = I_c$ ), respectively. Thus,

$$\prod_i (I_{ci} / I_{si}) = \prod_j (I_{cj} / I_{sj}). \quad (5)$$

Replacing in (5) the saturation current  $I_s$  by the product of the emitter area  $A$  and the geometry-independent saturation current density  $J_s$ , which can be assumed to be equal for all BJT of the same kind of conductivity (pnp or npn), we can write

$$\prod_i I_{ci} = \lambda \prod_j I_{cj} \quad \text{with} \quad \lambda = \left( \prod_i A_i \right) / \left( \prod_j A_j \right). \quad (6)$$

Thus, even in the case of large  $\lambda$ , the ratio of emitter areas can still remain moderate.

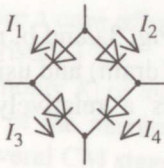


Fig. 1. Diode bridge.

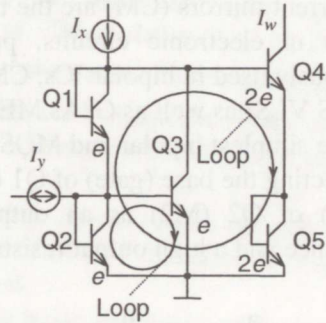


Fig. 2. Vector difference circuit.

For example, the vector difference circuit [1] in Fig. 2 involves two overlapping junction loops, which include emitter junctions of transistors Q2–Q3 and Q1–Q5, respectively ( $e$  is the unit emitter area). Therefore

$$I_{c2} = I_{c3}; \quad I_{c1} I_{c2} = (I_{c4} / 2)(I_{c5} / 2).$$

Including the vector currents produces

$$I_{c1} = I_x - I_{c3}, \quad I_{c2} = I_y + I_{c1}, \quad I_{c4} = I_{c5} = I_w,$$

from which we obtain

$$I_w = \sqrt{I_x^2 - I_y^2}.$$

Though the saturation current density of all transistors is not exactly the same (due to  $V_{be}$  mismatch, caused by mechanical stresses, temperature differences, or

local variations in junction doping), these problems can be surmounted by careful design, evidenced by high-precision ICs.

In general, translinear loops may include one or more voltage sources. Then from (4) and (6) follows

$$\left(\prod_i I_{ci}\right) / \left(\prod_j I_{cj}\right) = \lambda \exp(V_L / V_T), \quad (7)$$

where  $V_L$  is the sum of loop voltages, taking also into account the  $V_{be}$  mismatch of real components.

Translinear methods can also be used in MOS and CMOS circuits [8].

### 3. CURRENT MIRRORS

Current mirrors (CM) are the most significant primary current-mode building blocks in electronic circuits, particularly in all kinds of IC [1] circuitry. Previously used in bipolar ICs, CMs are now irreplaceable in modern nMOS and CMOS VLSI as well as GaAs MESFET structures.

The simplest bipolar and MOS CMs are shown in Fig. 3a and b, respectively. Connecting the base (gate) of Q1 (M1) to its collector (drain) and using collector (drain) of Q2 (M2) as an output of CM maintains a relatively low input resistance and a high output resistance of CM.

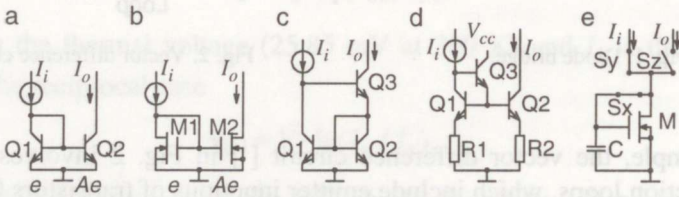


Fig. 3. Current mirrors: a–d, static; e, dynamic.

Several output transistors can be used. In order to enhance the output impedance, cascoded output stages are often applied.

Since the base-emitter (gate-source) voltage of Q2 (M2) is equal to that of Q1 (M1) and transistors are similar, their collector (drain) currents will also be equal to each other. In a general case, according to (6) the current gain  $K_I$  is approximately equal to the ratio  $A$  of emitter areas (channel widths) of transistors. Taking into account a finite value of  $\beta$ , for the CM in Fig. 3a we have

$$K_I = A / (1 + (1 + A) / \beta). \quad (8)$$

In order to diminish the gain error caused by  $\beta$  and to improve some other parameters, more complicated structures of CM are used. Wilson's CM in Fig. 3c has an improved accuracy gain  $K_I$

$$K_I = 1 - (2(\beta_1 - \beta_3) + 2) / (\beta_1\beta_3 + 2\beta_1 + 2), \quad (9)$$

but for different values of  $\beta$ , compensation of base currents is incomplete.

The configuration of Fig. 3d enables a more precise gain  $K_I$

$$K_I = A / (1 + (1/\beta_1 + A/\beta_2) / \beta_3) \quad (10)$$

and an improved output behaviour. However, both of them have a double input voltage drop.

In the case of tolerant transistors, the behaviour of CM can be improved using additional emitter resistors R1 and R2 (Fig. 3d). Since the voltage drops across resistors sufficiently exceed  $V_T$ , the gain of CM is determined by the ratio of resistances  $R_1/R_2$ , in the opposite case, by the ratio of the emitter areas  $A$ . If these two ratios are not equal, serious harmonic distortion of the signal may occur, like a case of parallel connecting of elements with linear and exponential characteristics [9].

Commonly  $K_I$  of less than 5 is chosen, while an increase in the gain leads to a decrease of the maximum operating frequency of CM. In order to obtain larger gains, several CM stages in series can be used.

Dynamic CMs (current copiers) with their basic structure, outlined in Fig. 3e, are widely used in modern, particularly low-voltage, analogue and digital systems. Transistor M is combined with three switches  $S_x$ ,  $S_y$ , and  $S_z$  that are implemented by means of additional transistors, and a capacitor C. In the first phase, M operates as the input device of a mirror. At the equilibrium state, capacitor C is charged to the voltage, corresponding to the current  $I_i$ . In the second phase, M operates as the output device and sinks an output current  $I_o$ , controlled by the same gate voltage, thus  $I_i = I_o$ . This simple circuit suffers from various limitations, and many improved and extended structures are in use.

For continuous current control of  $K_I$ , a differential CM structure (Fig. 4) with two inputs and two outputs is appropriate. In this case, the bias currents  $I_x$  and  $I_y$  can be determined separately and the current gain of CM is equal to  $I_y/I_x$ .

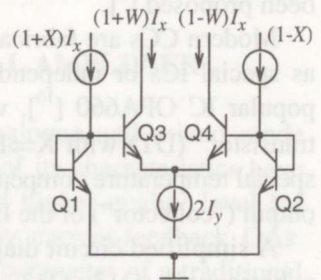


Fig. 4. Differential current mirror.

#### 4. CURRENT CONVEYOR

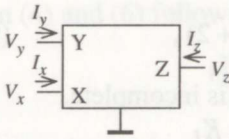


Fig. 5. Current conveyor.

A current conveyor (CC) in Fig. 5 is a four (five)-terminal device, which like a conventional operational amplifier (OA), in specific circuit configurations can perform many signal processing functions and simplify circuit design [1-5, 10, 11]. First introduced in 1968, it is only now that analogue IC designers have succeeded in creating a really outstanding new component. Main advantages of CC over conventional OA are a higher speed and a larger signal bandwidth.

For the CC of the first generation (CCI), if a potential is applied to input terminal Y, an equal potential will appear on the input terminal X. An input current  $I_X$  into X will result in an equal current flowing into Y as well as into output terminal Z, which behaves as a current source. Thus, the potential of X, being set by that of Y, is independent of the current of X. Similarly, the current of Y, being fixed by that of X, is independent of the voltage applied at Y. To increase the versatility of CC, a second generation (CCII) with a high impedance terminal Y was introduced that operates like an ideal transistor with infinite transconductance and input resistance. If the currents of Y and Z both are flowing into the CC, it is denoted by "+", in the opposite case, by "-". The CC can be described by the hybrid expression (Fig. 5)

$$\begin{bmatrix} I_Y \\ V_X \\ I_Z \end{bmatrix} = \begin{bmatrix} 0 & N & 0 \\ 1 & 0 & 0 \\ 0 & \pm 1 & 0 \end{bmatrix} \begin{bmatrix} V_Y \\ I_X \\ V_Z \end{bmatrix}, \quad (11)$$

where  $N = 1$  for CCI and  $N = 0$  for CCII. Recently, a current-controlled CC has been proposed [4].

Modern CCs are fabricated using complementary bipolar or CMOS technology as special ICs or independent parts of current-feedback OAs. Let us consider a popular IC OPA660 [10], which includes a CCII+ device named as a "diamond transistor" (DT) with  $X \Rightarrow E$ ,  $Y \Rightarrow B$  and  $Z \Rightarrow C$ , a buffer (voltage follower), and a special temperature compensating bias circuit. Connecting input of the buffer to the output ("collector") of the DT leads to a current-feedback OA.

A simplified circuit diagram of the IC is shown in Fig. 6. The DT consists of a basic unit (Q12, Q13, Q15, Q16), often used in power amplifiers [12], a complementary CM (Q17-Q20), and bias current sources (Q11, Q14). The latter two serve as outputs of the bias circuit that controls bias currents of the DT and buffer. Bias currents are predicted by  $R_q$  or  $I_q$ , varying of which enables a proper choice of main parameters, including the operation speed and maximum operating frequency of the IC.

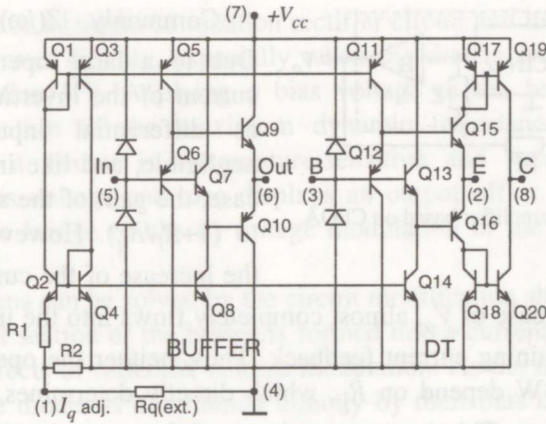


Fig. 6. IC OPA660 with diamond transistor and buffer.

The transconductance and input resistance of the DT can be expressed as

$$g_{ms} = g_{m12} + g_{m13}, \quad R_i = \beta^2 / g_{ms}, \quad (12)$$

where numbers in subscripts refer to respective transistors. For example,  $R_q = 250 \Omega$  yields:  $g_{ms} = 125 \text{ mS}$ ;  $R_i = 1 \text{ M}\Omega$ , while  $f_T = 700 \text{ MHz}$ .

Diamond structures (bipolar and CMOS) have a number of excellent features, such as high linearity and output current capability, high operating frequency and speed along with a simple control of parameters in a wide range. They are becoming a basic component for current-mode design. The DTs are often implemented as input stages of current-feedback OAs (CFOA), maintaining high slew rate and operating frequency.

## 5. CURRENT-FEEDBACK OPERATIONAL AMPLIFIER

An OA is a versatile basic building block for analogue and mixed mode electronic apparatus. Since its introduction, almost all of its characteristics have improved drastically. However, a completely new and higher quality level for some main dynamic parameters of OA is achieved by current-feedback OAs. They have an extremely high slew rate, exceeding the parameter of a traditional OA by more than one decade [1, 10, 11]. The large-signal bandwidth (BW) has also increased significantly, while small-signal BW over 1 GHz has been obtained.

Let us consider a non-inverting structure with the CFOA in Fig. 7. It can be seen that the connection of external elements is like that for the classical voltage-feedback OA.

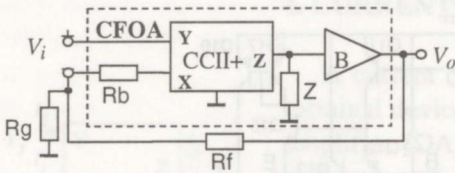


Fig. 7. Noninverting amplifier based on CFOA.

Commonly,  $|Z(j\omega)| \gg R_f \gg R_g$ .

Due to a large open-loop gain, the current of the inverting input as well as differential input voltage are negligible, and like in a conventional case, the gain of the structure is close to  $(1+R_f/R_g)$ . However, at  $R_g \gg R_b$ , the increase of the current through  $R_f$

caused by the increase of  $V_o$ , almost completely flows into the inverting input of the CFOA, maintaining current feedback. Thus, neither the open-loop gain nor the closed-loop BW depend on  $R_g$ , which directly determines the closed-loop gain of the structure. This is a new and one of the most significant features of CFOA-based amplifiers.

The analysis of the structure in Fig. 7 yields

$$K = (1 + R_f / R_g) / (1 + (1 + R_f / R_g)R_b / Z(s)). \quad (13)$$

Let, as usually,  $Z(s) = R/(1 + sRC_C)$ , where  $R$  is the value of  $Z(s)$  at  $f = 0$  and  $C_C$  is the corresponding parallel (correction) capacity. Then from (13)

$$BW = 1 / 2\pi C_C (R_f + (1 + R_f / R_g)R_b), \quad (14)$$

which in case of  $R_b \ll R_g$  yields:  $BW = 1/(2\pi C_C R_f)$ . Since the gain factor  $K$  is controlled by  $R_g$  while  $R_f$  and  $C_C$  are constant,  $BW$  is also approximately constant. Slew rate of the structure can be expressed as  $SR = V_o / C_C R_f$  and it has no conventional restrictions.

The open-loop gain of CFOA structures is often moderate, and therefore they have good stability. However, both DT and buffer, operating as current and voltage followers, respectively, have a deep internal negative feedback, maintaining for a given  $Z(t)$  an accurate gain of the structure.

An increasing number of different CFOAs based on complementary bipolar and CMOS technologies is available. Though some of their parameters, such as CMRR and offset voltage, are poorer than those for classical OA, they have improved sufficiently. On the other hand, new voltage-feedback OAs with diamond structures are now becoming available.

## 6. CURRENT-MODE RECTIFIERS WITH IMPROVED PRECISION

Rectification of low-level signals is critical and demanding in signal processing. The traditional approach based on diodes and OAs exhibits significant distortion during the zero-crossing of input signal, restricting the upper frequency limit of the circuit.



Development of a current summation rectifier circuit and its modifications [3] resulted in improved fidelity, especially when the diodes are prebiased to the edge of conduction [13]. Applying a bias voltage to the bridge results in a significant reduction of the maximum dynamic impedance of the diodes. However, such a circuit is temperature-sensitive and susceptible to small variations in bias voltage and also displays an output offset. Driving the load directly from the bridge results in voltage modulation of the current converter output terminals.

These problems can be solved by the circuit modification shown in Fig. 8 [14], where the output section of the bridge is formed into a current summation node, removing the effects of reflected voltage modulation. As the maximum dynamic resistance of the diodes is determined directly by their bias current rather than voltage, the bridge bias level is simply and accurately set as a current without problems of temperature or adjustment sensitivity. A single resistor returned to the voltage supply rail can generate the bias current in most cases. A separate circuit with similar diodes is required, along with a voltage-follower, to bias the main bridge. Current bias also permits the option of bias cancellation to minimize output offset.

According to (5), for the translinear bridge (Fig. 8)

$$I_1^2 - I_Z I_1 - (I_B/2)^2 = 0 \quad (15)$$

and output current,  $I_o$  is expressed as

$$I_o = \sqrt{I_Z^2 + I_B^2} \quad (16)$$

Although the addition of bridge bias brings a significant benefit to waveform fidelity, it must inevitably influence linearity in the transition region, where  $I_Z$  becomes comparable to  $I_B$ . At low bias current, however, the effect is negligible. Complete bias cancellation at the output node would require a fast square-root differencing circuit, whereas satisfactory partial compensation can be obtained simply by subtracting a current  $I_B/2$ , using a fixed value resistance.

The configuration in Fig. 8 contains two uncorrelated offset voltages. The total output-offset voltage  $V_{off}$  can be written as

$$V_{off} = -R_2(I_B \pm (V_{off1} \pm V_{off2})/r_d) \pm V_{off1}, \quad (17)$$

where  $R_2$ ,  $I_B$  are given in Fig. 8;  $V_{off1}$ ,  $V_{off2}$  are input-offset voltages of transimpedance amplifier and voltage follower, respectively;  $r_d = 2V_T/I_B$  is dynamic resistance of each bridge diode. At relatively large values of  $I_B$ , the last term in (17) can be ignored. However, for precise rectifiers with smaller  $I_B$ , this term can dominate.

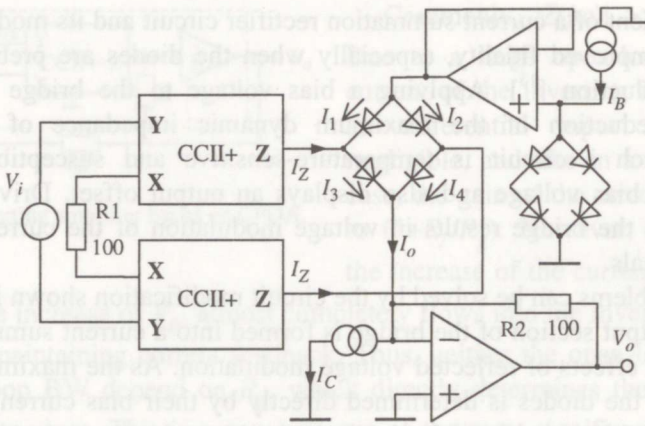


Fig. 8. Modified bridge using current bias.

The biasing method has been tested, using a number of different conveyor structures in the frequency region where the limitations of the zero-bias case are clearly evident. For example, the rectified low-level sinewave, obtained using AD844 ICs configured as conveyors with an AD847 transimpedance amplifier, showed noticeable distortion in the crossover region at 2 MHz. The waveshape was significantly improved when a bridge bias current of 40  $\mu\text{A}$  was applied.

The method is particularly suited to integration, promising very-high-speed precision rectifiers without any critical bias adjustments.

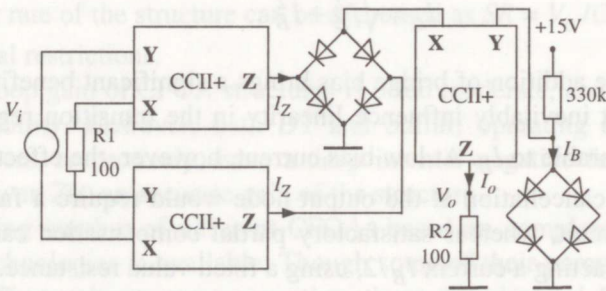


Fig. 9. New all-conveyor wideband precision rectifier.

A new all-conveyor approach is shown in Fig. 9 [15]. Combining the function of bias and output circuit together into a single CC leads to a significant improvement in the dynamic behaviour of the circuit. It also substantially simplifies the circuit configuration, and the unwanted output-offset voltage  $V_{off}$  will be reduced to

$$V_{off} = -R_2(I_B \pm V_{off1} / r_d), \quad (18)$$

where  $V_{off1}$  is the offset voltage of the CC.

The bias is transferred from the conveyor's Y-terminal to its X-terminal, which is directly connected to the signal bridge. Additionally, the signal bridge current flowing from the X-terminal is transferred to the conveyor's Z-terminal, thus providing an independent output which can be converted to a voltage through a load resistance or used for a further high efficient current-mode signal processing.

The circuit has been tested using both CCII01 and AD844 current conveyor ICs, with BAT85 Schottky diodes for the signal bridge and CA3096AE npn array transistors. A bridge bias current of approximately 45  $\mu\text{A}$  has been used to produce an optimum compromise between precision and speed.

Low-speed testing demonstrated an extremely good linearity. At frequencies up to 15 MHz, output-voltage offset was reduced from typically 60 mV to better than 20 mV with the new circuit. The peak rectified waveform imbalance was reduced from 50 to 5 mV.

The benefits to be derived from current-steering applied to diode bridges can be extended to include a number of other circuits. For example, the traditional design of chopper modulators widely employed in DSB-SC systems can also be designed around CCs.

Current-mode operation of diode-based circuits, in general, may be expected to bring operational benefits and enhanced circuit performance compared to their voltage-mode counterparts.

## 7. CONCLUSIONS

Ever increasing implementation of current-mode signal processing in various analogue as well as digital and mixed circuits and systems results from the following factors:

- bipolar and MOS transistors have a high output impedance, while their input impedances are rather low in some applications;
- modern IC technology is able to produce almost identical elements with similar characteristics, maintaining a good compensation of their non-linearity and temperature dependence;
- current signal processing can take place at very low supply voltages, and therefore reduced power consumption in highly dense circuits is achieved;
- recent developments in truly complementary bipolar technology have opened the door for the implementation of extremely linear and fast current-mode components such as diamond transistor and current-feedback amplifier.

As a consequence of new circuit ideas and modern IC processing technology, the current-mode building blocks, structures and systems can be characterized by good linearity, high operating speed and frequency, low power consumption, and low noise. They suit for modern technology coupled with the ever shrinking feature size of devices on ICs and the consequential reduction of power supply voltages.

## REFERENCES

1. Toumazou, C., Lidgley, F. J., and Haigh, D. G. (eds.). *Analogue IC Design: the Current-mode Approach*. Peter Peregrinus Ltd., London, 1990.
2. Wilson, B. Trends in current conveyor and current-mode amplifier design. *Int. J. Electronics*, 1992, **73**, 573–583.
3. Lidgley, F. J., Hayatleh, K., and Toumazou, C. New current-mode precision rectifiers. In *Proc. IEEE Int. Symp. on Circuits and Systems*. Chicago, USA, 1993, 1322–1325.
4. Fabre, A., Saaid, O., Wiest, F., and Boucheron, C. High frequency applications based on a new current controlled conveyor. *IEEE Trans. Circuits and Systems I: Fundamental Theory and Applications*, 1996, **43**, 82–91.
5. Männama, V. and Sabolotny, R. Modified PLL frequency synthesiser. In *Proc. 5th Biennial Baltic Electronics Conference, Oct. 7–11, 1996, Tallinn, Estonia*. Tallinn, 1996, 113–116.
6. Männama, V. A two-terminal current stabiliser. *USSR Author's Certificate No 1396812*, 1988 (in Russian).
7. Gilbert, B. Translinear circuits: a proposed classification. *Electron. Lett.*, 1975, **11**, 14–16.
8. Seevinck, E. and Wiegerink, R. J. Generalized translinear circuit principle. *IEEE J. Solid-State Circuits*, 1991, **26**, 1098–1102.
9. Männama, V. Complementary Darlington circuit. In *Proc. 4th Biennial Conference, Oct. 9–14, 1994, Tallinn, Estonia*. Tallinn, 1994, **1**, 223–228.
10. *Wide Bandwidth Operational Transconductance Amplifier OPA660*. Burr-Brown IC Data Book. Linear Products, 1994, 2296–2313.
11. Bruun, E. CMOS high speed, high precision current conveyor and current feedback amplifier structures. *Int. J. Electronics*, 1993, **74**, 93–100.
12. Tietze, V. and Schenk, C. *Electronic Circuits: Design and Applications*. 2nd ed. Springer-Verlag, Berlin, 1991.
13. Toumazou, C., Lidgley, F. J., and Chattong, S. High frequency current conveyor precision full-wave rectifier. *Electron. Lett.*, 1994, **30**, 745–746.
14. Wilson, B. and Männama, V. Current-mode rectifier with improved precision. *Electron. Lett.*, 1995, **31**, 247–248.
15. Wilson, B., Dodd, A. J., and Männama, V. All conveyor high-speed rectifier with improved precision and temperature stability. *Proc. Baltic Electronics Conference, Tallinn, Estonia*, 1996, 425–428.

## VOOLUTOIMELISED SIGNAALITÖÖTLUSLÜLITUSED

Vello MÄNNAMA

Artiklis on esitatud lühiülevaade voolutoimelise signaalitöötuse põhimõtetest ja nende rakendamisest nüüdisaegsete elektronlülituste projekteerimises. On selgitatud bipolaarstruktuurides kasutatavaid translineaarsuse printsiipe, staatiliste ja dünaamiliste voolupeeglite põhiomadusi, voolumuundurite töö teoreetilisi aluseid ning näidatud voolumuunduri realisatsiooni “teemantstruktuuriga” mikrolülitusena. Samuti on käsitletud voolutagasisidega operatsioonivõimendit kui mitmekülse rakendusega kiiret ja kõrge piirsagedusega elektronlülituste komponenti.

Seejärel on vaadeldud vooluprintsiibi rakendamist täppisalaldi dünaamiliste omaduste parandamiseks. On analüüsitud täppisalaldi silla modifitseeritud nihkeahelat, mis kõrvaldab tundlikkuse seaderežiimi suhtes, ning voolutoimelist sildalaldit. Lõpuks on kirjeldatud voolumuunduritega laiaribalise alaldi täiustatud struktuuri, mis on kasutatav ka kiirete balanssmodulaatorite korral.